Structural, magnetic, and Mössbauer spectral study of Er_2Fe_{17} and its hydrides

F. Grandjean*
Institute of Physics, B5, University of Liège, B-4000 Sart-Tilman, Belgium

O. Isnard†
Laboratoire de Cristallographie, associé à l'Université J. Fourier et à l'INPG, CNRS, F-38042 Grenoble, France

Dimitri Hautot and Gary J. Long‡
Department of Chemistry, University of Missouri-Rolla, Rolla, Missouri 65409-0010

(Received 25 May 2000; revised manuscript received 10 August 2000; published 11 December 2000)

The structural and magnetic properties of the $Er_2Fe_{17}H_x$ compounds, where x is 0, 1, 2, 3, and 3.8, have been investigated by means of powder x-ray diffraction, thermal and ac magnetic susceptibility measurements, and iron-57 Mössbauer spectroscopy. The $Er_2Fe_{17}H_x$ compounds crystallize in the hexagonal $P6_3/mmc$ space group with the Th_2Ni_{17}-like structure, a structure which has both an iron-rich stoichiometry and disorder of the erbium and iron–iron $4f-4f$ dumbbell sites. The increase in the lattice parameters, the magnetic ordering temperature, the saturation magnetization, and the dependence of the Mössbauer spectral hyperfine parameters upon the hydrogen content reveal a two-step filling of the interstitial sites, with hydrogen first filling the octahedral $6h$ sites for $x<3$ and then partially filling the tetrahedral $12i$ sites for $x=3$ and 3.8. Neither the Mössbauer spectra nor the ac magnetic susceptibility measurements reveal any spin reorientation in any of these compounds. In all of the compounds both the excess amount of iron and the expected disorder is confirmed by the Mössbauer spectra and the hyperfine parameters of the iron $4e$ site are reported herein. Finally, the Mössbauer spectra indicate that the interstitial hydrogen atoms partially occupying the tetrahedral $12i$ sites are jumping between these sites on the Mössbauer time scale.

DOI: 10.1103/PhysRevB.63.014406 PACS number(s): 76.80.+y, 75.50.Bb, 75.50.−y

I. INTRODUCTION

The insertion of interstitial hydrogen into the crystal structure of a compound generally induces dramatic changes in its physical, electronic, and magnetic properties. Further, for intermetallic magnetic compounds, either hydrogen decrepitation[1] or hydrogen decomposition desorption and recombination,[2,3] yield small magnetic particles which are very useful in the manufacture of new high performance permanent magnets.

Ferromagnetic iron rich $R_2Fe_{14}B$ and R_2Fe_{17} compounds, where R is a rare-earth, have been shown[4–7] to absorb large amounts of hydrogen, an absorption that leads to hydrides which are stable at ambient temperature and pressure. Many interesting changes have been observed upon the insertion of interstitial hydrogen into the various R_2Fe_{17} compounds, changes which include a modification of the crystal field experienced by the rare-earth,[8] an increase in the magnetization,[7,9] and even, in some cases, an increase in the magnetic ordering temperature.[7]

The R_2Fe_{17} compounds with the lighter rare-earth atoms are found to crystallize in the rhombohedral $R\text{-}3m$ space group with the Th_2Zn_{17}-like structure. In contrast, for the heavier rare-earth atoms the R_2Fe_{17} compounds crystallize in the hexagonal $P6_3/mmc$ space group with the Th_2Ni_{17}-like structure; the change usually occurs at gadolinium and results from the lanthanide contraction with increasing rare-earth atomic number. Typically the rhombohedral compounds are very close to or exactly stoichiometric and have completely ordered crystal structures. In contrast, the hexagonal compounds can be either stoichiometric or nonstoichiometric, usually with a rare-earth deficiency, and/or can have disordered crystal structures.

Detailed Mössbauer spectral studies have been reported[10–13] on R_2Fe_{17}, where R is Ce, Pr, Nd, and Gd, and their hydrides, all of which have the ordered rhombohedral structure, and on Dy_2Fe_{17} and its hydrides,[14] which have the disordered hexagonal structure. Both a slowing down of the jumping of hydrogen between the partially occupied tetrahedral $18g$ sites and a magnetic spin reorientation have recently been discovered[10,15] in $Pr_2Fe_{17}H_x$ through Mössbauer spectral studies. In contrast, no such slowing down or magnetic spin reorientation is observed[11,14] in either $Nd_2Fe_{17}H_x$ or $Dy_2Fe_{17}H_x$. The existence of a spin reorientation in $Pr_2Fe_{17}H_x$, for x greater than 2, has been attributed[10,15] to the positive Steven's coefficient, γ_J, of praseodymium.

Because erbium, as well as samarium and holmium, has a positive[16] Steven's coefficient, α_J, it is expected that a change in chemical composition, the application of pressure or a magnetic field, could induce a spin reorientation in Er_2Fe_{17}. Indeed, a spin reorientation has been observed in the $Er_2Fe_{17}C_y$ interstitial carbides[17–19] with $y>1$, in $Er_2Fe_{17}N_3$,[20–23] and in the pseudobinary $Er_2Fe_{17-x}M_x$ compounds,[24–26] where M is Mn, Co, and Ga. In all of these compounds, the magnetization rotates away from the c axis toward the basal plane with increasing temperature; the temperature at which this spin reorientation occurs is sensitive to the amount, y, of interstitial carbon or nitrogen or to the amount, x, of metal substitution and is typically between 100 and 295 K. Because of the sensitivity of the spin-reorientation temperature to chemical composition, complex compositions,[21,27,28] such as $Er_2Fe_{17}C_yN_z$ and

$Er_2Fe_{17-x}Al_xN_y$, have been studied. Pressure[29,30] induced and magnetic field[31–33] induced spin reorientations have also been observed in Er_2Fe_{17}.

Because Er_2Fe_{17} and its hydrides crystallize[7] in the hexagonal $P6_3/mmc$ space group, they exhibit atomic disorder, a disorder which was first reported[34] in 1969 for Er_2Fe_{17} and is most likely comparable to that found[6] in Ho_2Fe_{17}. This disorder manifests[34] itself as an additional substitution of erbium by $4e$ iron dumbbell atom pairs. Also, because both Steven's coefficients, α_J and γ_J, are positive for erbium[16] a search for a spin reorientation in the hydrides of Er_2Fe_{17} is worthwhile. Further, because of the lanthanide contraction across the series of $R_2Fe_{17}H_x$ compounds, the maximum number of interstitial hydrogen atoms in Er_2Fe_{17} is 3.8 and not 5 as is found[10,15] in $Pr_2Fe_{17}H_x$. This partial filling of the tetrahedral interstitial $12i$ hydrogen site may also influence the dynamic nature of hydrogen in $Er_2Fe_{17}H_{3.8}$ and $Er_2Fe_{17}D_{3.8}$.

For the above reasons we present herein an x-ray diffraction, magnetic, and Mössbauer spectral study of the $Er_2Fe_{17}H_x$ compounds, where x varies from 0 to 3.8 and of $Er_2Fe_{17}D_{3.8}$.

II. EXPERIMENT

Polycrystalline Er_2Fe_{17} was prepared[6,9] by melting, in a high frequency induction furnace, purer than 99.95 percent metals placed in a cold copper crucible under a purified argon atmosphere. In order to optimize the sample homogeneity, small pieces of the resulting ingot were wrapped in tantalum foil, sealed in an evacuated silica tube, and annealed at 1270 K for at least two weeks. Because the starting ingot composition was slightly rich in iron, the actual ingot composition was $Er_2Fe_{17.5}$. This latter composition completely agrees with the homogeneity range of the Er_2Fe_{17} phase found[34] in the Er–Fe phase diagram. Further, the homogeneity range of R_2Fe_{17}, where R is a heavy rare earth is also known[35] to broaden with increasing rare-earth atomic number.

The hydrogenation of $Er_2Fe_{17.5}$ to form $Er_2Fe_{17.5}H_{3.8}$ was performed at 373 K in a stainless steel autoclave under a hydrogen pressure of ca. 5 MPa. The hydrogen content was controlled by measuring the change in hydrogen vapor pressure in the autoclave and was determined by gravimetric analysis. The accuracy of the hydrogen content is estimated to be ± 0.1 hydrogen atoms per formula unit, an accuracy which has been confirmed[10,36] in related R_2Fe_{17} compounds through neutron diffraction studies. The preparation of $Er_2Fe_{17}D_{3.8}$ was carried out in a similar fashion by replacing hydrogen with deuterium. Samples with an intermediate hydrogen concentration were obtained by heating the appropriate mixture of $Er_2Fe_{17.5}$ and $Er_2Fe_{17.5}H_{3.8}$ in a sealed tube. In order to both promote hydrogen diffusion and to optimize the sample homogeneity, the sample was heated three times from room temperature to 570 K over a period of 2 to 3 hours. The resulting homogeneity was checked by conventional x-ray powder diffraction with iron $K_{\alpha 1}$ radiation. In all cases no Bragg peaks corresponding to α-iron were observed in the x-ray diffraction pattern and no sextet corresponding to α-iron was observed in the Mössbauer spectra.

High accuracy lattice parameters have been obtained with a Guinier-type focusing camera and a monochromatic x-ray beam containing only iron $K_{\alpha 1}$ radiation. Powdered silicon was added to the sample as an internal lattice parameter standard. The diffraction pattern was recorded on x-ray film which was subsequently scanned with a 20 μm step in order to extract the relative diffraction intensities. The indexation of the Bragg peaks was carried out for a hexagonal unit cell, a cell which is compatible with the hexagonal $P6_3/mmc$ space group. The lattice parameters were then obtained by a least squares refinement which used 25 observed Bragg reflections, a refinement which leads to an accuracy of ca. ± 0.002 Å for both the a and c lattice parameters.

The magnetic ordering temperatures have been determined with a Faraday torque balance at a heating and cooling rate of 5 K per minute. A sample of ca. 50 to 100 mg was sealed under a vacuum in a small silica tube in order to prevent oxidation of the sample during heating. The saturation magnetization of Er_2Fe_{17} and $Er_2Fe_{17}H_{3.8}$ was determined[37] at 5 K by the extraction method in a continuous field of up to 7 T. The 4.2 to 295 K ac magnetic susceptibility has been determined with a computer controlled mutual inductance susceptometer[38] which used an exciting field of 1 Oe at a frequency of 120 Hz. A lock-in amplifier has been used to measure the complex susceptibility, $\chi_{ac}=\chi'-j\chi''$, where χ' is the initial susceptibility and is related to the variation in the magnetization of the sample and χ'' is nonzero when magnetic energy is absorbed by the sample.

Mössbauer spectral absorbers of ca. 36 mg/cm^2 were prepared from powdered samples which had been sieved to a 0.045 mm or smaller diameter particle size. The Mössbauer spectra have been obtained between 4.2 and 295 K on a constant-acceleration spectrometer which utilized a rhodium matrix cobalt-57 source and was calibrated at room temperature with α-iron foil. The studies were carried out in a Janis Supervaritemp cryostat in which the samples were never exposed to a vacuum. The spectra have been fit as discussed below and the estimated errors are at most ± 1 kOe for the hyperfine fields, ± 0.002 mm/s for the isomer shifts, and ± 0.005 mm/s for the quadrupole shifts.

III. STRUCTURAL AND MAGNETIC RESULTS

Structural properties. The complex disordered hexagonal Th_2Ni_{17}-like structure with the $P6_3/mmc$ space group, adopted by the R_2Fe_{17} compounds, where R is a heavy rare-earth element, has been extensively discussed[14] in our previous paper on Dy_2Fe_{17}. The reader should consult Fig. 1 of Ref. 14 for details of the substitutional disorder of the rare earth by dumbbell iron–iron pairs, a disorder which has been confirmed by high resolution neutron diffraction studies[6,39,40] of Ho_2Fe_{17}, by x-ray diffraction studies[40,41] of Lu_2Fe_{17} and Y_2Fe_{17}, and by single crystal neutron diffraction studies[39,40] of Tm_2Fe_{17} and Lu_2Fe_{17}. The observed degree of disorder is known to depend upon the method of preparation and/or upon the initial stoichiometry of the preparative mixture. Unfortunately, it is very difficult to determine the degree of

TABLE I. Structural parameters and magnetic ordering temperatures for $Er_2Fe_{17}H_x$.[a]

$Er_2Fe_{17}H_x$	a, Å	c, Å	V, Å^3	$\Delta V/x$, Å^3/atom	T_c, K
Er_2Fe_{17}	8.431(1)	8.280(2)	509.7(3)		315(5)
$Er_2Fe_{17}H$	8.455(2)	8.293(2)	513.5(4)	1.9	378(4)
$Er_2Fe_{17}H_2$	8.484(2)	8.298(2)	517.2(4)	1.9	428(4)
$Er_2Fe_{17}H_3$	8.520(1)	8.310(1)	522.4(2)	2.1	482(4)
$Er_2Fe_{17}H_{3.8}$	8.540(2)	8.321(2)	525.5(4)	2.1	498(4)

[a]The corresponding error bars are given in parentheses.

disorder from powder x-ray diffraction studies on Er_2Fe_{17}. Hence, because the sample of Er_2Fe_{17} studied herein was prepared by a method essentially identical to that of Ho_2Fe_{17}, it is reasonable to assume that the degree of disorder is the same in the two compounds. Thus, the nominal Er_2Fe_{17} stoichiometry is best represented by $Er_2Fe_{17.5}$ and the statistical occupations of the $2b$, $2c$, and $2d$ rare-earth sites are 75.6, 16.0, and 100 percent, respectively, and the statistical occupations of the $4e$ and $4f$ iron dumbbell sites are 24.4 and 84.0 percent, respectively; the remaining iron sites are fully occupied. The lattice parameters and the unit-cell volume of Er_2Fe_{17} are given in Table I and they agree very well with previously published[34,35] values.

Hydrogen content. The lattice parameters and unit cell volumes of $Er_2Fe_{17}H_x$, which crystallize in the $P6_3/mmc$ space group, are given in Table I. The maximum amount of hydrogen which can be inserted into Er_2Fe_{17} was found to be 3.8 hydrogen atoms per formula unit, a value which is consistent with those reported,[6,7] for rare-earth atoms of similar size, i.e., for $Ho_2Fe_{17}H_x$. The 3.8 hydrogen atoms are significantly less than the five atoms which can be inserted into the rhombohedral R_2Fe_{17} compounds formed with lighter rare-earth atoms such as Ce, Pr, Nd, Sm, or Gd.

Neutron diffraction experiments[6,36] indicate that two different interstitial sites can accommodate hydrogen, the octahedral $6h$ sites, which are most favored by hydrogen and the tetrahedral $12i$ sites which are located near the rare-earth atoms. For rare-earth atoms heavier than gadolinium, the maximum amount of hydrogen is smaller than for the lighter rare-earth atoms because of the effect of the lanthanide contraction upon the volume of the interstices and because of the rare-earth stoichiometric deficiency and the preference of hydrogen to bond with the rare-earth atoms. Figure 1 indicates a close to linear correlation between the maximum hydrogen content and the R_2Fe_{17} unit-cell volume. As shown in this figure, Ce_2Fe_{17} seems to be an exception to this correlation, most likely because of the tendency of the valence state of cerium to approach the tetravalent state.

Compositional dependence of the lattice parameters. The lattice parameters and unit-cell volumes of the $Er_2Fe_{17}H_x$ compounds are given in Table I. The a lattice parameter increases linearly with a slope of 0.0294 Å per hydrogen atom in $Er_2Fe_{17}H_x$, a slope which is larger than the values of 0.0265 and 0.0281 observed[10,14] in $Dy_2Fe_{17}H_x$ and $Pr_2Fe_{17}H_x$, respectively. The c lattice parameter also increases linearly with x with a slope of 0.0103 Å per hydrogen atom. The linear increase with x between zero and 3.8 is different than the sharp nonlinear increase observed[10,14] in the c parameter for x greater than 3 in both $Dy_2Fe_{17}H_x$ and $Pr_2Fe_{17}H_x$. The insertion of hydrogen into the Er_2Fe_{17} lattice induces a linear increase of the unit-cell volume with a slope of 2.1 Å^3 per hydrogen atom.

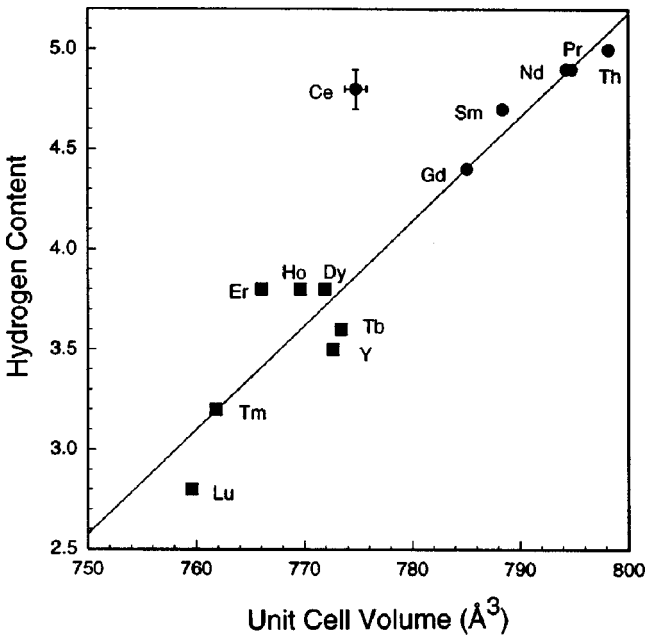

FIG. 1. The maximum hydrogen content as a function of the R_2Fe_{17} unit-cell volume. The hexagonal and rhombohedral compounds are designated by ● and ■, respectively. For comparison purposes the hexagonal unit-cell volumes have been multiplied by 1.5. Error bars are shown only for Ce_2Fe_{17} but are similar for all the remaining compounds. Data obtained in part from Ref. 7.

Previous structural studies of $R_2Fe_{17}H_x$, where R is Ce, Pr, Nd, Gd, and Dy, have indicated[10–15,36] that the hydrogen atoms occupy the interstitial sites in two stages, first, the octahedral sites and second, the tetrahedral sites, stages which are similar for both the rhombohedral and the hexagonal structures. This two stage occupation is clearly indicated by the discontinuity in the compositional dependence of the lattice parameters and unit cell volume at x greater than 3. No such discontinuity is observed for $Er_2Fe_{17}H_x$. The absence of any discontinuity may result from the lanthanide contraction and the consequent partial filling of the tetrahedral site by hydrogen in $Er_2Fe_{17}H_x$ at x values less than 3. As will be noted below, this hypothesis is confirmed by the compositional dependence of the Mössbauer hyperfine parameters.

Magnetic ordering temperature. The magnetic ordering temperatures, T_c, of the $Er_2Fe_{17}H_x$ compounds, for $x \geqslant 1$, obtained from thermomagnetic measurements, see Fig. 2, and of Er_2Fe_{17} obtained from the Mössbauer spectral study, see below, are given in Table I. It should be noted that, for some unknown reason, the ordering temperature of Er_2Fe_{17}, as determined from the ac susceptibility measurements, see Fig. 3(a) is lower by ca. 20 K than the value reported in Table I. As is indicated in Table I, T_c increases linearly with a slope of 55.1 K per hydrogen atom in $Er_2Fe_{17}H_x$ for x

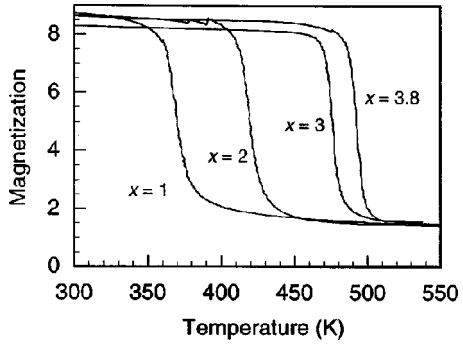

FIG. 2. The temperature dependence of the magnetization of $Er_2Fe_{17}H_x$.

values between 0 and 3 and then increases by only 16 K for a further 0.8 increase in x. The increase in T_c observed upon hydrogen insertion is a common feature[42] of the R_2Fe_{17} compounds, a feature which is related, at least in part, to the unit cell expansion, an expansion which favors ferromagnetic exchange interactions. The compositional dependence of T_c observed herein for $Er_2Fe_{17}H_x$ is very similar to that reported[14] for the $Dy_2Fe_{17}H_x$ compounds and confirms that hydrogen insertion on the tetrahedral 12*i* sites is less effective in increasing T_c than is insertion on the octahedral 6*h* sites. This interpretation is also supported by the positive correlation[43] between the iron–iron interatomic distance within the iron dumbbell and the occupancy of the octahedral 6*h* sites by hydrogen.

Saturation magnetization and ac susceptibility. The saturation magnetization at 5 K is 17.9 and 17.1 μ_B per formula unit for Er_2Fe_{17} and $Er_2Fe_{17}H_{3.8}$, respectively. The value of 17.9 μ_B per formula unit obtained for Er_2Fe_{17} is in good agreement with the previously measured[44] value. Because of the decrease at higher temperatures of the antiferromagnetic contribution of the erbium sublattice to the magnetization, the saturation magnetization of $Er_2Fe_{17}H_{3.8}$ increases to 23.6 μ_B per formula unit at 295 K.

Both components of the ac magnetic susceptibility for Er_2Fe_{17}, $Er_2Fe_{17}H_2$, $Er_2Fe_{17}H_3$, and $Er_2Fe_{17}H_{3.8}$ are shown as a function of temperature in Fig. 3. The corresponding curves for $Er_2Fe_{17}H$ are similar to those of $Er_2Fe_{17}H_2$. The dramatic drop in the ac magnetic susceptibility of Er_2Fe_{17} is associated with the ferrimagnetic to paramagnetic transition at ca. 295 K. As mentioned above, previous studies have revealed that carbon[17,19] and nitrogen[20,21] insertion or Mn, Co, or Ga substitution for iron[24–26] in Er_2Fe_{17} and hydrogen insertion[10] into rhombohedral Pr_2Fe_{17} induces a magnetic spin reorientation. Thus ac susceptibility measurements have been performed on the $Er_2Fe_{17}H_x$ compounds in order to search for a similar spin reorientation. This technique is known[45] to be very sensitive to changes in the magnetization direction in rare-earth and transition-metal intermetallic compounds. In the case of the hydrides a smooth shoulder is observed in the real portion, χ', of the ac susceptibility centered at ca. 120, 125, 90, and 60 K for $x=1$, 2, 3, and 3.8, respectively. However no anomaly in the imaginary portion, χ'', of the ac susceptibility is associated with this shoulder, indicating that no absorption of magnetic energy is associated with the shoulder, an absorption of energy which is expected if there is as a spin reorientation at these temperatures. Hence, the shoulder in the real portion of the ac susceptibility is not related to a spin reorientation. The absence of a spin reorientation is also confirmed by the Mössbauer spectral results, see below, and is consistent with the decrease[8] in the crystal field at the rare-earth nucleus upon hydrogenation. However, the shoulder observed in the real portion, χ', of the ac susceptibility is reminiscent of the anomaly reported[46–49] in several $R_2Fe_{14}B$ compounds, in Sm_2Fe_{17}, and in $CeFe_2$, and associated with a magnetic after

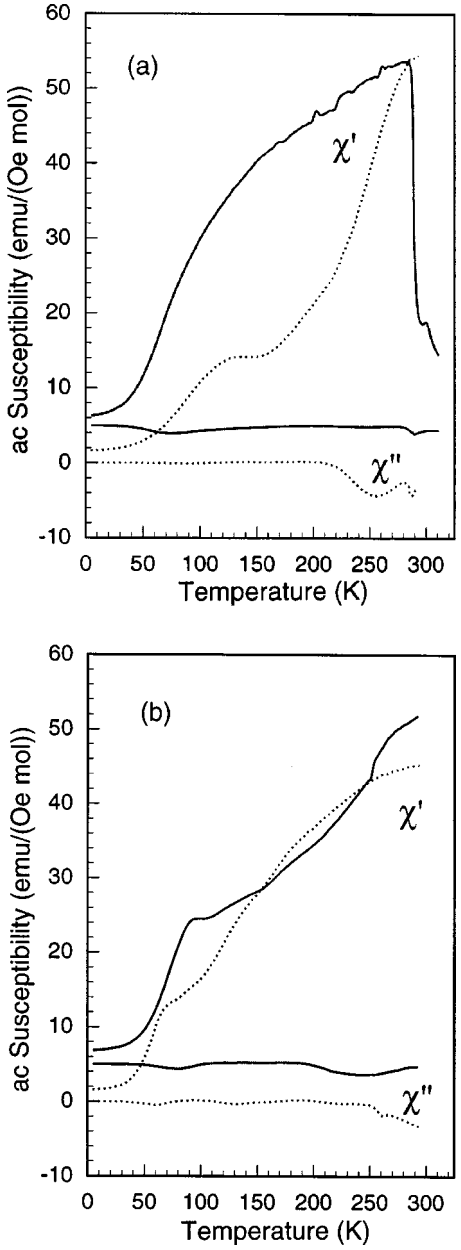

FIG. 3. The temperature dependence of the real, χ', and the imaginary, χ'', portions of the ac magnetic susceptibility of Er_2Fe_{17}, solid lines, and $Er_2Fe_{17}H_2$, dashed lines (a) and $Er_2Fe_{17}H_3$, solid lines, and $Er_2Fe_{17}H_{3.8}$, dashed lines (b). To avoid overlap 5 emu/(Oe mol) has been added to the values for Er_2Fe_{17} and $Er_2Fe_{17}H_3$.

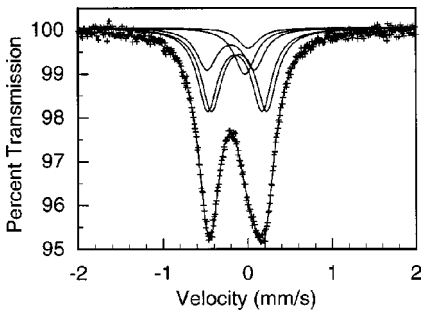

FIG. 4. The 320 K Mössbauer spectrum of Er_2Fe_{17}.

effect. The fundamental nature of this anomaly is not understood at this time.

IV. MÖSSBAUER SPECTRAL RESULTS

The Mössbauer spectra of Er_2Fe_{17}, obtained between 4.2 and 320 K, are shown in Figs. 4–6. Recently, very poor quality Mössbauer spectra[21] of Er_2Fe_{17}, obtained between 18 and 310 K, have been analyzed in terms of a model which ignores the structural disorder in Er_2Fe_{17}. This disorder introduces[14] a total of five crystallographically inequivalent iron sites, i.e., the $4e$, $4f$, $6g$, $12j$, and $12k$ sites. The Mössbauer spectra of Er_2Fe_{17} indicate that T_c is 315 ± 5 K. The high resolution 320 K Mössbauer spectrum of Er_2Fe_{17}, see Fig. 4, permits a detailed spectral analysis which was not possible with the earlier poorly resolved[21] spectrum at 310 K. A fit with four symmetric doublets of relative areas 4:6:12:12, assigned to the $4f$, $6g$, $12j$, and $12k$ sites, respectively, failed to fit the inner side of the line at 0.2 mm/s. The missing absorption is clearly an indication of iron occupation of the $4e$ site. Indeed, as is shown in Fig. 4, a fit with five symmetric doublets with relative areas of 4.4, 10.1, 17.1, 34.2, and 34.2 percent, assigned to the $4e$, $4f$, $6g$, $12j$, and $12k$ sites, respectively, is excellent; the corresponding hyperfine parameters are given in Table II. It is clear that several

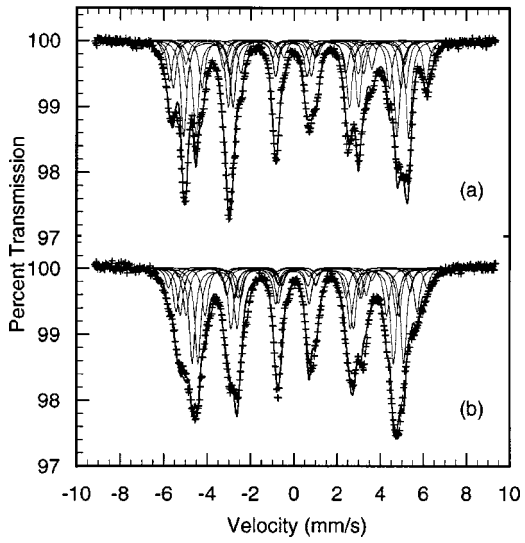

FIG. 5. The 4.2 K Mössbauer spectra of Er_2Fe_{17} (a) and $Er_2Fe_{17}H_{3.8}$ (b).

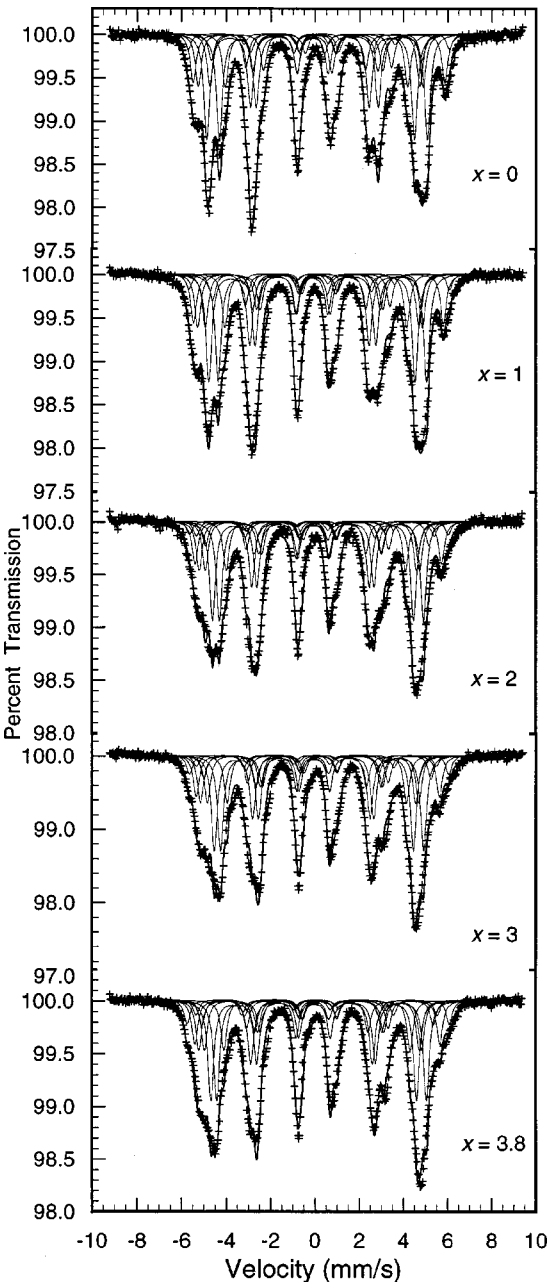

FIG. 6. The 85 K Mössbauer spectra of $Er_2Fe_{17}H_x$.

satisfactory alternative fits of this spectrum can be obtained with five symmetric doublets. However, the fit shown in Fig. 4 agrees with the fit[13] of the paramagnetic spectrum of Ce_2Fe_{17} and, further, the resulting isomer shifts and quadrupole splittings are consistent with the corresponding parameters obtained below the ordering temperature, see below.

The 4.2 K spectrum, shown in Fig. 5, agrees well with the earlier spectrum obtained[50] at 15 K. Because of the point symmetry of the five iron sites and the basal orientation of the magnetization in Er_2Fe_{17}, there are eight magnetically inequivalent iron sites, i.e., the $4e$, $4f$, $6g_4$, $6g_2$, $12j_8$, $12j_4$, $12k_8$, and $12k_4$ sites. In the earlier Mössbauer spectral study[50] of Er_2Fe_{17}, the disorder was ignored and an additional subdivision of the $12j$ site was used, a subdivision which was based upon a calculation[51] of the dipolar fields in

TABLE II. Mössbauer spectral hyperfine parameters for $Er_2Fe_{17}H_x$.

	x	T, K	$4f$	$4e$	$6g_4$	$6g_2$	$12j_8$	$12j_4$	$12k_8$	$12k_4$	Wt. Avg.
H, kOe	0	4.2	367	385	333	313	322	285	288	290	315
		85	352	365	314	294	308	272	273	276	300
		295	144	165	110	98	112	71	72	71	98
	1	85	349	364	314	291	304	298	275	254	298
		295	242	264	208	195	204	201	178	157	198
	2	85	344	362	308	312	295	295	271	250	293
		295	275	307	240	245	232	232	209	192	230
	3	85	340	362	305	317	292	291	269	251	295
		295	285	307	254	262	244	239	223	203	244
	3.8	4.2	345	370	313	325	303	301	280	260	304
		85	342	366	311	323	301	300	279	260	302
		295	290	303	257	270	255	262	235	215	255
δ,[a] mm/s	0	4.2	0.185	0.195	−0.035	−0.035	0.048	0.048	0.000	0.000	0.039
		85	0.175	0.190	−0.035	−0.035	0.033	0.033	−0.010	−0.010	0.029
		295	−0.040	0.020	−0.145	−0.145	−0.100	−0.100	−0.140	−0.140	−0.110
		320	−0.030	0.010	−0.200	−0.200	−0.100	−0.100	−0.150	−0.150	−0.121
	1	85	0.158	0.205	−0.028	−0.028	0.034	0.034	−0.010	−0.010	0.028
		295	0.010	0.070	−0.150	−0.150	−0.080	−0.080	−0.125	−0.125	−0.092
	2	85	0.150	0.195	−0.040	−0.040	0.040	0.040	0.010	0.010	0.031
		295	0.040	0.075	−0.135	−0.135	−0.070	−0.070	−0.090	−0.090	−0.073
	3	85	0.140	0.195	−0.008	−0.008	0.061	0.061	0.039	0.039	0.057
		295	0.02	0.065	−0.100	−0.100	−0.055	−0.055	−0.062	−0.062	−0.051
	3.8	4.2	0.140	0.180	0.015	0.015	0.070	0.070	0.050	0.050	0.087
		85	0.135	0.165	0.015	0.015	0.065	0.065	0.050	0.050	0.066
		295	0.030	0.070	−0.060	−0.060	−0.035	−0.035	−0.045	−0.045	−0.031
QS,[b] mm/s	0	4.2	−0.050	−0.020	−0.310	0.220	0.135	0.620	0.250	−0.530	
		85	−0.050	−0.020	−0.310	0.220	0.135	0.620	0.200	−0.530	
		295	0.010	−0.020	−0.420	0.140	0.180	0.600	0.040	−0.420	
		320	0.040	0.040	−0.560		0.655		−0.644		
	1	85	−0.100	0.020	−0.340	0.260	0.230	−0.280	0.210	0.140	
		295	−0.100	0.020	−0.340	0.260	0.220	−0.320	0.170	0.180	
	2	85	−0.100	0.020	−0.380	0.330	0.240	−0.400	0.160	0.100	
		295	−0.100	0.020	−0.380	0.330	0.200	−0.400	0.160	0.200	
	3	85	−0.020	0.020	−0.430	0.270	0.270	−0.400	0.130	0.120	
		295	−0.020	0.020	−0.400	0.210	0.210	−0.400	0.210	0.170	
	3.8	4.2	−0.020	0.040	−0.400	0.270	0.270	−0.350	0.100	0.120	
		85	−0.020	0.040	−0.400	0.270	0.260	−0.350	0.100	0.140	
		295	−0.020	0.040	−0.400	0.150	0.230	−0.320	0.120	0.140	
Area, %	0		10.60	3.35	11.47	5.74	22.94	11.47	22.94	11.47	
	1		10.60	3.40	11.45	5.72	22.90	11.45	22.90	11.45	
	2		9.98	3.17	11.58	5.79	23.16	11.58	23.16	11.58	
	3		9.95	4.55	11.40	5.70	22.80	11.40	22.80	11.40	
	3.8		10.10	5.38	11.36	5.78	22.78	11.36	22.78	11.36	

[a]The isomer shifts are given relative to room temperature α-iron foil.

[b]QS are the quadrupole shift values, except for Er_2Fe_{17} at 320 K, where QS are quadrupole splitting values.

Y_2Fe_{17}. However, it seems that the calculated orientation of the dipolar field which gives rise to this additional subdivision is not compatible with the orientation of the magnetization in the basal plane of Er_2Fe_{17}. Hence, the fits shown in Figs. 5(a) and 6 have been obtained with eight magnetic sextets assigned to the $4e$, $4f$, $6g_4$, $6g_2$, $12j_8$, $12j_4$, $12k_8$, and $12k_4$ sites in Er_2Fe_{17}.

The line shape, the width, and the relative area of the absorption at the highest velocity in Figs. 5(a) and 6 indicate the presence of iron on the $4e$ site. The usual constraint on

the equality of the isomer shifts of the crystallographically equivalent and magnetically inequivalent sites has been used in all of these fits. Further, one linewidth of 0.31 mm/s at 4.2 K and of 0.32 mm/s at all the remaining temperatures was used for all components in the spectra. The hyperfine parameters resulting from the fits at 4.2, 85, and 295 K, as well as the relative areas of the sextets, are given in Table II. Because of the atomic disorder discussed above, the relative areas of the spectral components of the iron $4e$, $4f$, $6g$, $12j$, and $12k$ sites, are expected,[6] on the basis of the disorder observed for Ho_2Fe_{17}, to be 2.84, 9.79, 17.47, 34.95, 34.95 percent, respectively. Even though these relative areas have not been constrained to these values, the best fit values agree reasonably with these expected values.

Between 4.2 and 320 K the $4e$ iron site is characterized by the largest isomer shift, as is expected for a site which shows the same $3m$ local symmetry as that of the $4f$ site and has a larger Wigner–Seitz cell volume. Among the remaining isomer shifts, see Table II, the $4f$ isomer shift is the largest and the $6g$ isomer shift is the smallest, values which are in agreement both with the results obtained[10,13,52–57] on the R_2Fe_{17} compounds, where R is Y, Ce, Pr, Nd, Sm, Tb, and Th, and with their respective Wigner–Seitz cell volumes. The sequence of hyperfine fields, $4e>4f>6g>12j>12k$, at all temperatures, is also identical, with the exception of the addition of the $4e$ site, to the sequence observed[10,13,52–57] for the R_2Fe_{17} compounds, where R is Y, Ce, Pr, Nd, Sm, Tb, and Th. Further, this sequence agrees with that of the number of iron near neighbors, $10=10>9=9>8$. It should be noted that the iron–iron dumbbell distance is typically longer[6,39] in the $4e$ than in the $4f$ site, a longer distance which favors ferromagnetic exchange and increases the hyperfine field.

The 4.2 K Mössbauer spectrum of $Er_2Fe_{17}H_{3.8}$ and the 85 K spectra of the $Er_2Fe_{17}H_x$ compounds are shown in Figs. 5 and 6, respectively. It is clear that the Mössbauer spectra of the hydrides show less detail than those of Er_2Fe_{17}. The presence of a sextet with a large hyperfine field, the sextet which gives rise to an absorption line at the extreme right of the 85 K spectra, see Fig. 6, is a clear signature of the sextet assigned to the $4e$ site and arising from the structural disorder. Hence, the spectra of the hydrides have also been fit with an eight sextet model, as was the case for Er_2Fe_{17}. One linewidth of 0.32 mm/s was used for all spectra. The resulting hyperfine parameters and relative areas of the eight sextets are also given in Table II and their temperature dependence is discussed below. The relative areas of the hydride sextets, see Table II, indicate that there is little, if any, hydrogen compositional dependence of the atomic disorder. Because of the method used to prepare the hydrides, the same atomic disorder and excess iron stoichiometry are expected in all of the compounds.

The temperature dependence of the five isomer shifts in $Er_2Fe_{17}H_x$ follow the expected second order Doppler shift and that of the weighted average for Er_2Fe_{17} and $Er_2Fe_{17}H_{3.8}$ is shown in Fig. 7. The solid lines in Fig. 7 are the result of a least squares fit[58] with a Debye model for the second order Doppler shift and the fits correspond to Debye temperatures of 265 and 360 K, and effective vibrating masses of 57 and

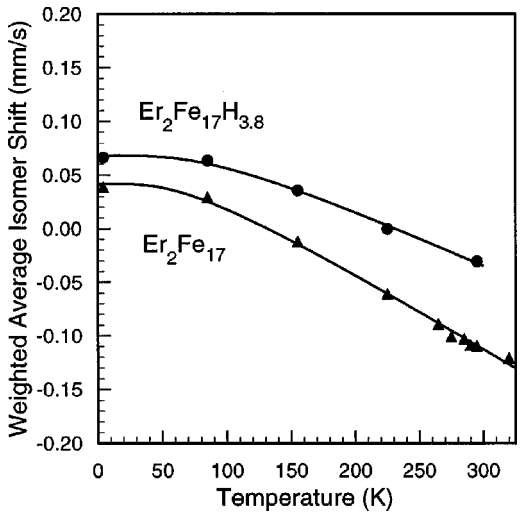

FIG. 7. The temperature dependence of the weighted average isomer shifts in Er_2Fe_{17} and $Er_2Fe_{17}H_{3.8}$. The solid lines are the result of least squares fits with a Debye model. The error bars are approximately the size of the data points.

75 g/mol, for Er_2Fe_{17} and $Er_2Fe_{17}H_{3.8}$, respectively. These values indicate that the lattice of $Er_2Fe_{17}H_{3.8}$ is more rigid and tightly bound than the lattice of Er_2Fe_{17}, no doubt because of the insertion of hydrogen into the lattice and the added covalency which results.

The compositional dependence of the 85 K isomer shifts of $Er_2Fe_{17}H_x$, where x is 0, 1, 2, 3, and 3.8, is shown in Fig. 8. In all the compounds, the $4e$ and $4f$ sites have the largest isomer shifts and the $6g$ site has the smallest isomer shift, values which are in agreement with the results obtained[10–14] on the hydrides of R_2Fe_{17}, where R is Ce, Pr, Nd, Sm, Gd, and Dy. The $4e$ and $4f$ isomer shifts show little variation with x, probably because of the smaller expansion of the lattice along the c axis as compared to the larger expansion along the a axis. The $6g$, $12j$, and $12k$ isomer shifts increase

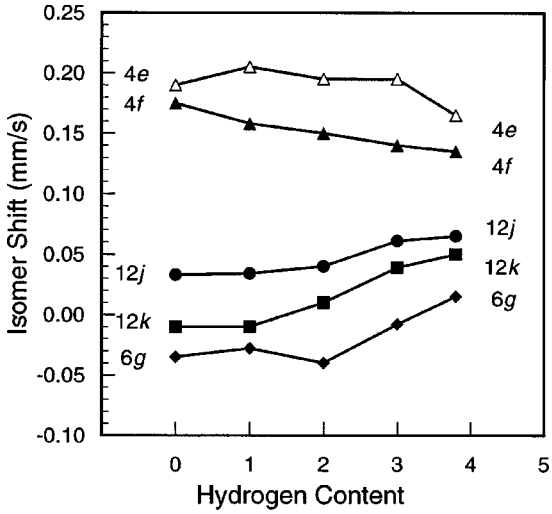

FIG. 8. The compositional dependence of the 85 K isomer shifts in $Er_2Fe_{17}H_x$. The error bars are approximately the size of the data points.

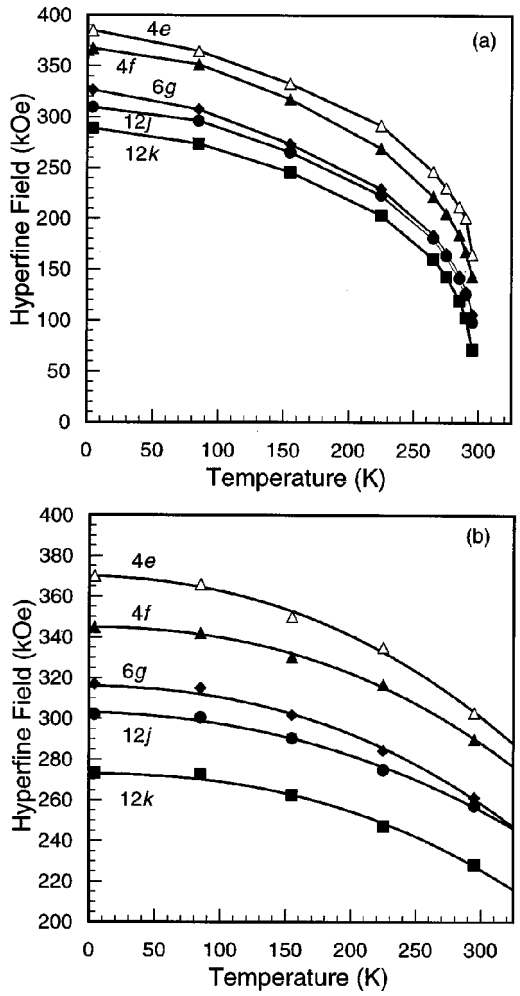

FIG. 9. The temperature dependence of the site weighted average hyperfine fields in Er_2Fe_{17} (a) and $Er_2Fe_{17}H_{3.8}$ (b). The error bars are approximately the size of the data points.

with increasing x in agreement with the lattice expansion upon hydrogen insertion and the presence of near-neighbor hydrogen atoms for the 12j and 12k sites. A slightly more substantial increase in the 6g, 12j, and 12k isomer shifts was observed[14] in the $Dy_2Fe_{17}H_x$ compounds. This slight difference between the two series of compounds is likely to result from the lattice contraction along the lanthanide series. As is shown in Fig. 8, the 6g, 12j, and 12k isomer shifts are markedly larger for x equal to 3 and 3.8, than for x less than 3. This increase is believed to result from the filling of the tetrahedral 12i sites by hydrogen, a filling which has begun to occur even for x equal to 3.

The temperature dependence of the site weighted average hyperfine fields is shown in Figs. 9(a) and 9(b) for Er_2Fe_{17} and $Er_2Fe_{17}H_{3.8}$, respectively. The other hydrides shown similar Brillouin-type behavior for their hyperfine fields. The sequence of hyperfine fields, $4e>4f>6g>12j>12k$, is identical to the sequence observed in the hydrides[10–14] of R_2Fe_{17}, where R is Ce, Pr, Nd, Sm, Gd, and Dy, and agrees with the decrease in the number of iron near neighbors, $10=10>9=9>8$.

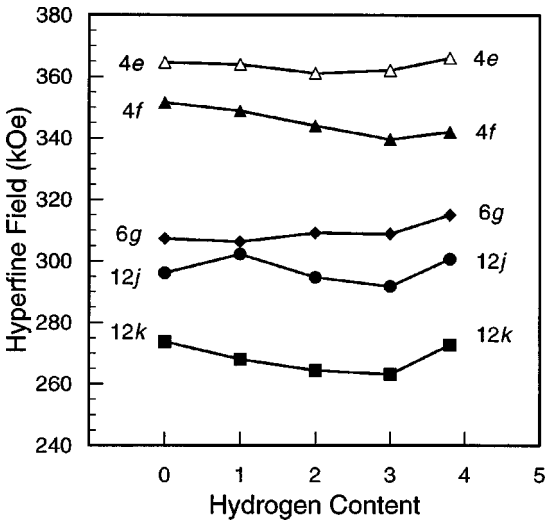

FIG. 10. The compositional dependence of the 85 K site weighted average hyperfine fields in $Er_2Fe_{17}H_x$. The error bars are approximately the size of the data points.

The solid lines in Fig. 9(b) are the result of a least squares fit[59] with the equation,

$$H=H_0[1-B_{3/2}(T/T_C)^{3/2}-C_{5/2}(T/T_C)^{5/2}], \qquad (1)$$

where H_0 and T_C are the saturation field and the magnetic ordering temperature, respectively. The $T^{3/2}$ term in this equation has its origin[60] in the excitations of long-wavelength spin waves. The $B_{3/2}$ coefficients vary between 0.06 and 0.13 for the five sites in $Er_2Fe_{17}H_{3.8}$, values which are comparable to the values of 0.11 and 0.12 observed[61] for α-iron and nickel and indicate spin waves of similar wavelength. In the fits shown in Fig. 9(b) the $T^{5/2}$ term is unusually large with $C_{5/2}$ coefficients of ca. 0.4. These large coefficients probably arise because of the proximity of the magnetic ordering temperature. Indeed, the equation is known to be most applicable at temperatures well below the ordering temperature. This limited applicability range also prevents the application of this equation to the temperature dependence of the fields in Er_2Fe_{17}, fields which are shown in Fig. 9(a). A plot of the reduced weighted average hyperfine field versus the reduced temperature for Er_2Fe_{17} follows quite closely a Brillouin curve for $S=3/2$.

There is relatively little variation in the 85 K hyperfine fields with hydrogen content as is indicated in Fig. 10, except for the small increases in the fields for $x=3.8$. This increase is no doubt a result of the filling of the 12i sites by hydrogen.

The 4.2 K spectrum of $Er_2Fe_{17}H_{3.8}$, see Fig. 5, indicates that the interstitial hydrogen atoms which partially occupy the interstitial 12i sites are jumping between these sites on the Mössbauer time scale of ca. 10^{-7} s. If these interstitial hydrogen atoms were static on this time scale, the 12k sites would be divided into eight sites with one tetrahedral interstitial hydrogen near neighbors and four sites with no tetrahedral interstitial hydrogen near neighbors and the sextet assigned to the 12k site would have to be subdivided into two sextets with a two to one area ratio. Such a subdivision of the 12k sextet is not necessary to obtain an excellent fit of the

4.2 K spectrum and we conclude that, even at 4.2 K, there is no evidence that the tetrahedral interstitial hydrogen becomes static on the Mössbauer time scale, a behavior which is similar to the dynamic behavior observed[10,11,14] in $Pr_2Fe_{17}H_4$, $Nd_2Fe_{17}H_5$, and $Dy_2Fe_{17}H_{3.8}$.

V. CONCLUSIONS

In Ce_2Fe_{17}, Pr_2Fe_{17}, Nd_2Fe_{17}, and Dy_2Fe_{17} the increase in the *c* lattice parameter with increasing hydrogen content reflects the filling of the tetrahedral interstitial sites with hydrogen atoms. In Er_2Fe_{17}, this increase is more subtle and suggests that the filling of the tetrahedral 12*i* sites in disordered hexagonal Er_2Fe_{17} begins at slightly less than three hydrogen atoms per formula unit because both the lanthanide contraction and the excess iron stoichiometry hamper the filling of some of the interstitial octahedral 6*h* sites. This suggestion is also supported by the compositional dependence of the isomer shifts in $Er_2Fe_{17}H_x$.

The insertion of hydrogen in Er_2Fe_{17} increases the magnetic ordering temperature as well as the saturation magnetization; the enhancement of the magnetization is more significant at room temperature because of the increase in the ordering temperature. Both ac susceptibility and Mössbauer spectral results indicate that, in contrast to carbon or nitrogen insertion or metal substitution, hydrogen insertion does not induce a spin-reorientation in Er_2Fe_{17}. Further, because of atomic disorder, the Mössbauer spectral fits require a specific sextet which is assigned to iron occupying the 4*e* site and is characterized by hyperfine parameters very similar to those of the 4*f* site, an assignment which is in agreement with the identical site symmetry of the two sites and the identical near-neighbor environments and similar bond distances of the two sites.

Because the hydrides $Pr_2Fe_{17}H_x$, with $x \geqslant 3$, show an axial magnetization below their spin-reorientation temperature and the hydrides $Dy_2Fe_{17}H_x$ and $Er_2Fe_{17}H_x$ do not, it would be interesting to investigate the rear-earth solid solutions, $Pr_{2-y}Dy_yFe_{17}H_x$ and $Pr_{2-y}Er_yFe_{17}H_x$ for the existence of a spin reorientation.

ACKNOWLEDGMENTS

This research was supported in part by the U.S. National Science Foundation through Grants Nos. DMR95-21739 and INT-9815138, and through a NATO Cooperative Scientific Research Grant No. CRG 961088. The support of the CNRS–NSF No. 7418 action initiative is greatly acknowledged. Travel funds from the ''Fonds National de la Recherche Scientifique, Brussels, Belgium'' are also greatly appreciated.

*Electronic address: fgrandjean@ulg.ac.be
†Electronic address: isnard@labs.polycnrs-gre.fr
‡Electronic address: glong@umr.edu

[1] R. Fruchart, R. Madar, A. Rouault, Ph. L'héritier, P. Taunier, D. Fruchart, and P. Chaudouet, EU Patent No. 85 401230.9.
[2] T. Takeshita, J. Alloys Compd. **193**, 231 (1993).
[3] D. Book and I. R. Harris, IEEE Trans. Magn. **MAG-28**, 2145 (1992).
[4] D. Fruchart, L. Pontonnier, F. Vaillant, J. Bartolomé, J. M. Fernandez, K. A. Puertolas, C. Rillo, J. R. Regnard, A. Yaouanc, R. Fruchart, and P. L'héritier, IEEE Trans. Magn. **MAG-24**, 1641 (1988).
[5] W. X. Zhong, K. Donnelly, J. M. D. Coey, B. Chevalier, J. Etourneau, and T. Berlureau, J. Mater. Sci. **23**, 329 (1988).
[6] O. Isnard, S. Miraglia, J. L. Soubeyroux, D. Fruchart, and A. Stergiou, J. Less-Common Met. **162**, 273 (1990).
[7] O. Isnard, S. Miraglia, J. L. Soubeyroux, D. Fruchart, and P. L'héritier, J. Magn. Magn. Mater. **137**, 151 (1994).
[8] O. Isnard, P. Vulliet, A. Blaise, J. P. Sanchez, S. Miraglia, and D. Fruchart, J. Magn. Magn. Mater. **131**, 83 (1994).
[9] O. Isnard, S. Miraglia, D. Fruchart, and J. Deportes, J. Magn. Magn. Mater. **103**, 23 (1992).
[10] D. Hautot, G. J. Long, F. Grandjean, O. Isnard, and S. Miraglia, J. Appl. Phys. **86**, 2200 (1999).
[11] F. Grandjean, G. J. Long, S. Mishra, O. A. Pringle, O. Isnard, S. Miraglia, and D. Fruchart, Hyperfine Interact. **95**, 571 (1995).
[12] D. Hautot, G. J. Long, F. Grandjean, O. Isnard, and D. Fruchart, J. Magn. Magn. Mater. **202**, 107 (1999).
[13] D. Hautot, G. J. Long, F. Grandjean, and O. Isnard, Phys. Rev. B **62**, 11 731 (2000).
[14] O. Isnard, D. Hautot, G. J. Long, and F. Grandjean, J. Appl. Phys. **88**, 2750 (2000).
[15] F. Grandjean, D. Hautot, G. J. Long, O. Isnard, S. Miraglia, and D. Fruchart, J. Appl. Phys. **85**, 4654 (1999).
[16] K. H. J. Stevens, Proc. Phys. Soc., London, Sect. A **65**, 209 (1952).
[17] J. P. Liu, F. R. de Boer, P. F. de Chatel, and K. H. J. Buschow, Phys. Rev. B **50**, 3005 (1994).
[18] R. J. Zhou, Cz. Kapusta, M. Rosenberg, and K. H. J. Buschow, J. Alloys Compd. **184**, 235 (1992).
[19] B. G. Shen, L. Cao, L. S. Kong, T. S. Ning, and M. Hu, J. Appl. Phys. **75**, 6256 (1994).
[20] Y. Xu, T. Ba, and Y. Liu, J. Appl. Phys. **73**, 6937 (1993).
[21] K. G. Suresh and K. V. S. Rama Rao, Phys. Rev. B **55**, 15 060 (1997).
[22] P. C. M. Gubbens, A. A. Moolenaar, G. J. Boeder, A. M. van der Kraan, T. H. Jacobs, and K. H. J. Buschow, J. Magn. Magn. Mater. **97**, 69 (1991).
[23] B. P. Hu, H. S. Li, H. Sun, J. F. Lawler, and J. M. D. Coey, Solid State Commun. **76**, 587 (1990).
[24] N. P. Thuy, J. Zukrowski, H. Figiel, J. Przewoznik, and K. Krop, Hyperfine Interact. **40**, 441 (1988).
[25] R. Kumar and W. B. Yelon, J. Appl. Phys. **67**, 4641 (1990).
[26] B. G. Shen, Z. H. Cheng, H. Tang, B. Liang, S. Y. Zhang, F. W. Wang, W. S. Zhan, F. R. de Boer, and K. H. J. Buschow, Solid State Commun. **107**, 781 (1998); B. G. Shen, Z. H. Cheng, B. Liang, H. Q. Guo, J. X. Zhang, H. Y. Gong, F. W. Wang, Q. W. Yan, and W. S. Zhan, Appl. Phys. Lett. **87**, 1621 (1995).
[27] X. C. Kou, R. Groessinger, M. Katter, J. Wecker, L. Schultz, T. H. Jacobs, and K. H. J. Buschow, J. Appl. Phys. **70**, 2272 (1991).
[28] F. M. Yang, N. Tang, J. L. Wang, X. P. Zhong, R. W. Zhao, and W. G. Lin, J. Appl. Phys. **75**, 6241 (1994).

[29] J. Kamarad, O. Mikulina, Z. Arnold, B. Garcia-Landa, M. R. Ibarra, and P. A. Algarabel, J. Magn. Magn. Mater. **196–197**, 701 (1999).
[30] J. Kamarad, O. Mikulina, Z. Arnold, B. Garcia-Landa, and M. R. Ibarra, J. Appl. Phys. **85**, 4874 (1999).
[31] R. Verhoef, F. R. de Boer, S. Sinnema, J. J. M. Franse, F. Tomiyama, M. Ono, M. Date, and A. Yamagishi, Physica B **177**, 223 (1992).
[32] B. Garcia-Landa, P. A. Algarabel, M. R. Ibarra, F. E. Kayzel, T. H. Ahn, and J. J. M. Franse, J. Magn. Magn. Mater. **140–144**, 1085 (1995); B. Garcia-Landa, M. R. Ibarra, P. A. Algarabel, F. E. Kayzel, T. H. Ahn, and J. J. M. Franse, Physica B **177**, 227 (1992).
[33] X. C. Kou, F. R. de Boer, R. Groessinger, G. Wiesinger, H. Suzuki, H. Kitazawa, T. Takamasu, and G. Kido, J. Magn. Magn. Mater. **177–181**, 1002 (1998).
[34] A. V. van der Groot and K. H. J. Buschow, J. Less-Common Met. **21**, 151 (1970); K. H. J. Buschow and A. V. van der Groot, Phys. Status Solidi **35**, 515 (1969).
[35] K. H. J. Buschow, J. Less-Common Met. **11**, 204 (1966).
[36] O. Isnard, S. Miraglia, J. L. Soubeyroux, and D. Fruchart, Solid State Commun. **87**, 13 (1992).
[37] A. Barlet, J. C. Genna, and P. Lethuillier, Cryogenics **31**, 801 (1991).
[38] C. Rillo, F. Lera, A. Badia, L. Angurel, J. Bartolomé, F. Palacio, R. Navarro, and A. J. Duyneveldt, in *Susceptibility of Superconductors and Other Spin Systems*, edited by R. A. Hein, J. L. Francavilla, and D. H. Liebenberg (Plenum, New York, 1992).
[39] D. Givord and R. Lemaire, C. R. Seances Acad. Sci., Ser. B **274**, 1166 (1972); D. Givord, Ph.D. thesis, Université de Grenoble, 1973; B. Kebe, Ph.D. thesis, Université de Grenoble, 1983.
[40] D. Givord, R. Lemaire, J. M. Moreau, and E. Roudaut, J. Less-Common Met. **29**, 361 (1972).
[41] A. N. Christensen and R. G. Hazell, Acta Chem. Scand. **A34**, 455 (1980).
[42] O. Isnard, S. Miraglia, and D. Fruchart, J. Magn. Magn. Mater. **140–144**, 981 (1995).
[43] O. Isnard, J. L. Soubeyroux, S. Miraglia, D. Fruchart, L. M. Garcia, and J. Bartolomé, Physica B **180–181**, 629 (1992).
[44] E. E. Alp, A. M. Umarji, S. K. Malik, G. K. Shenoy, M. Q. Huang, E. B. Boltich, and W. E. Wallace, J. Magn. Magn. Mater. **68**, 305 (1987).
[45] F. J. Lazaro, L. M. Garcia, F. Luis, J. Bartolomé, D. Fruchart, O. Isnard, S. Miraglia, S. Obbade, and K. H. J. Buschow, J. Magn. Magn. Mater. **101**, 372 (1991).
[46] L. M. Garcia, J. Bartolomé, F. J. Lazaro, C. De Francisco, J. M. Munoz, and D. Fruchart, J. Magn. Magn. Mater. **140–144**, 1049 (1995).
[47] J. Bartolomé, L. M. Garcia, F. J. Lazaro, Y. Grincourt, L. G. De la Fuente, C. De Francisco, J. M. Munoz, and D. Fruchart, IEEE Trans. Magn. **30**, 577 (1994).
[48] S. Miraglia, J. L. Soubeyroux, C. Kolbeck, O. Isnard, D. Fruchart, and M. Guillot, J. Less-Common Met. **171**, 51 (1991).
[49] E. H. Büchler, M. Hirsher, and H. Kronmüller, in *Interstitial Intermetallic Alloys*, edited by G. J. Long, F. Grandjean, and K. H. J. Buschow (Kluwer, Dordrecht, 1994), p. 521.
[50] B. P. Hu, H. S. Li, H. Sun, and J. M. D. Coey, J. Phys.: Condens. Matter **3**, 3983 (1991).
[51] W. Steiner and R. Haferl, Phys. Status Solidi A **42**, 739 (1977).
[52] G. J. Long, O. A. Pringle, F. Grandjean, and K. H. J. Buschow, J. Appl. Phys. **72**, 4845 (1992).
[53] G. J. Long, O. A. Pringle, F. Grandjean, W. B. Yelon, and K. H. J. Buschow, J. Appl. Phys. **74**, 504 (1993).
[54] G. J. Long, O. A. Pringle, F. Grandjean, T. H. Jacobs, and K. H. J. Buschow, J. Appl. Phys. **75**, 2598 (1994).
[55] F. Grandjean, G. J. Long, O. A. Pringle, and K. H. J. Buschow, Hyperfine Interact. **94**, 1971 (1994).
[56] G. J. Long, S. Mishra, O. A. Pringle, F. Grandjean, and K. H. J. Buschow, J. Appl. Phys. **75**, 5994 (1994).
[57] S. R. Mishra, G. J. Long, O. A. Pringle, G. K. Marasinghe, D. P. Middleton, K. H. J. Buschow, and F. Grandjean, J. Magn. Magn. Mater. **162**, 167 (1996).
[58] G. J. Long, D. Hautot, F. Grandjean, D. T. Morelli, and G. P. Meisner, Phys. Rev. B **60**, 7410 (1999).
[59] H. N. Ok, K. S. Baek, and C. S. Kim, Phys. Rev. B **24**, 6600 (1981).
[60] C. Herring and C. Kittel, Phys. Rev. **81**, 869 (1951).
[61] B. E. Argyle, S. H. Charap, and E. W. Pugh, Phys. Rev. **132**, 2051 (1963).